

Article

Effect of Triclosan and Silver Nanoparticles on DNA Damage Investigated with DNA-Based Biosensor

Jana Blaškovičová * and Ján Labuda

Faculty of Chemical and Food Technology, Institute of Analytical Chemistry, Slovak University of Technology, Radlinského 9, 812 37 Bratislava, Slovakia; jan.labuda@stuba.sk

* Correspondence: jana.blaskovicova@stuba.sk

Abstract: Triclosan (TCS) is a broad-spectrum antimicrobial agent widely used in personal care, healthcare, and clinical practice. One of the most important aspects of toxicological profiling of compounds is their interaction with DNA. In human cells, TCS causes a significant reduction in DNA methylation. The involvement of TCS in chromosomal aberrations, DNA damage, and strand breaks, as well as DNA damage from TCS degradation products, was reported. AgNPs share similarities with TCS in terms of antimicrobial properties, enter the body after exposure, and are used even together with TCS in oral care products. Therefore, their mutual effect on the DNA is of interest. In this study, the electrochemical behavior of TCS on a glassy carbon electrode (GCE) and the biosensor with salmon sperm dsDNA (DNA/GCE), DNA damage by TCS present in phosphate buffer solution pH 7.4 and an additional effect of the immobilized AgNP layer on such DNA damage have been investigated. Two different sizes of AgNPs (about 15 and 37 nm) were tested. Using square-wave voltammetric signals of nucleobases, the portion of survived DNA was 64% in the presence of 15 nm AgNPs compared to 55% in its absence. The protective effect of AgNPs on DNA against TCS-induced DNA damage was found.



Citation: Blaškovičová, J.; Labuda, J. Effect of Triclosan and Silver Nanoparticles on DNA Damage Investigated with DNA-Based Biosensor. *Sensors* **2022**, *22*, 4332. <https://doi.org/10.3390/s22124332>

Academic Editors: Martina Medvidović-Kosanović, Anamarija Stanković, Ivana Novak Jovanović and Géza Nagy

Received: 3 May 2022

Accepted: 6 June 2022

Published: 8 June 2022

Publisher's Note: MDPI stays neutral with regard to jurisdictional claims in published maps and institutional affiliations.



Copyright: © 2022 by the authors. Licensee MDPI, Basel, Switzerland. This article is an open access article distributed under the terms and conditions of the Creative Commons Attribution (CC BY) license (<https://creativecommons.org/licenses/by/4.0/>).

Keywords: DNA-based biosensor; silver nanoparticles; triclosan

1. Introduction

Triclosan (TCS), 5-chloro-2-(2,4-dichlorophenoxy) phenol, is a broad-spectrum of antibacterial, antiviral, and antifungal agent frequently used as a preservative during the past 45 years in pharmaceuticals, personal care products, and cosmetics including toothpaste [1], soaps, shampoos, skin cleansers, detergents, deodorants, skin care lotions and creams [2], fabric and plastic additives [3,4], and impregnated in numerous different materials ranging from athletic clothing to food packaging [5]. TCS has also been used in surgical scrubs and in hand washing prior to surgery, to eradicate microorganisms such as methicillin-resistant *Staphylococcus aureus* (MRSA) [5]. In 1997, the FDA approved the use of TCS (0.3%) in Colgate Total toothpaste to prevent gingivitis and cavities. At the widespread use of TCS, it entered the environment and its presence in waters and waste waters in the US and Europe has been reported [2,6,7]. TCS has been detected in aquatic organisms, and sediments [8,9]. Significant levels of TCS are detected in body fluids in all age groups [5]. TCS has been detected in urine, plasma, serum and breast milk in humans all over the world [10–12]. TCS can accumulate in the human body, [13] where a large portion of free TCS is localized within the liver [14]. The prevalence of TCS exposure was indicated among youth [15].

Due to the bioaccumulation of TCS and its resistance to degradation, it represents a wide hazard to health. Hepatocellular adenomas and carcinomas were found in mice after exposure to TCS [16], additionally it enhanced liver fibrogenesis and tumorigenesis in mice [17]. Various toxic effects of TCS have been observed in studies affecting the nervous system [18–20], reproductive and developmental system [21,22], immune system, also at

disruption of the endocrine system [23], thyroid hormone homeostasis [5], disturbance of the intestinal microbiota [24], antibiotic resistance [5,25,26], potential carcinogenicity [27], and neurotoxicity [28]. Recent data showed that TCS was associated with allergies and hay fever [29]. TCS can interfere with hormone regulation and fat metabolism that could cause hormone dyshomeostasis, induction of oxidative stress, apoptosis, and inflammation [30].

The widespread use of silver nanoparticles (AgNPs) in daily products shows great potential due to their effective biocidal activities [31,32]. AgNPs are the most widely used engineered nanoparticles in commercial products such as cosmetics, food, and medicine [33,34]. They share similarities with TCS in terms of antimicrobial properties, microbiome disruption, implications for antibiotic resistance, and effects on opportunistic pathogens [35]. At the same time, AgNPs as an alternative to TCS differ from TCS in structural properties, toxicity mechanisms, and bioavailability. AgNPs in toothpaste, mouthwashes [36], and other products such as impregnated toothbrushes and cosmetic products for the care of enamel remineralization and dental hypersensitivity could be responsible for inflammation of the gastrointestinal tract [37–39]. The nanoscale size range allows the entry of particles and directly affects intracellular structures [40]. Cellular uptake of engineered nanoparticles is often size dependent [41]. They persist in different organs up to several months. The accumulation of AgNPs decreases significantly with increasing size [42]. Furthermore, the retention of AgNPs was longer within a higher dose of smaller nanoparticles [43].

The antimicrobial effects of AgNPs depend on structural factors such as size, shape, coating, and ion release [44–46]. Biocompatibility and stability increases with a decrease in AgNPs size due to the higher surface-area-to-volume ratio [47–49]. The antibacterial activity of AgNPs smaller than 10 nm is mainly due to an Ag⁺ release [50]. The colloidal morphology has higher antibacterial activity when compared to other morphologies [51,52]. AgNPs-induced neurotoxicity could be reflected in irreversible degenerate spatial cognition [53,54]. A deep transdermal distribution of AgNPs was observed inside the body, followed by prolonged exposure [55]. However, even more alarming is the accumulation of TCS in body fluids by rapid absorption through the skin and gastrointestinal tract [56–58]. Therefore, concomitant exposure of the organism to TCS and AgNPs and their mutual effect on the DNA is of interest.

One of the most important aspects of the toxicological profiling of various compounds is their interaction with the DNA molecules [59]. TCS causes a significant reduction in DNA methylation in human cells [60]. An increase in dose-responsive chromosomal aberrations [16] and DNA damage [6,61] was observed with exposure to TCS but also to AgNPs [62]. The interaction of drugs and small species such as nanoparticles with DNA structure was investigated by electrochemical DNA-based biosensors, which became a very viable alternative due to high sensitivity in the detection of small differences in double helix structure compared to other methods [63,64]. Recently, the mechanisms of direct DNA damage caused by TCS degradation products was thoroughly investigated on a large scale of pH from 3.4 to 12.04 using a DNA-based biosensor [65]. At the interaction in solution of 0.1 M acetate buffer of pH 4.5; the condensation of double helix chain was found to lead to the difficulty of nitrogenous bases oxidation on the surface of the glassy carbon electrode (GCE) as well as the release of guanine moiety [65].

The novelty of our study is to contribute and characterize a prevention of DNA toward harmful chemicals such as TCS using another potentially protective DNA substance. Such an approach is known in the chemistry of immobilized species, including the construction of structured materials and biosensors. With respect to the known association of AgNPs with dsDNA [66], these nanoparticles of two different sizes, namely Ag1NPs (15 nm) and Ag2NPs (37 nm), were selected for this study. To prevent acidic or basic DNA denaturation, in this study the physiological pH value (0.1 mol·L⁻¹ phosphate buffer solution at pH 7.4, PB) was used. The DNA damage by TCS was investigated using the DNA/GCE and AgNPs/DNA/GCE biosensors.

2. Materials and Methods

2.1. Materials

Triclosan (TCS), 5-chloro-2-(2,4-dichlorophenoxy)phenol, and low molecular weight salmon sperm double helix DNA were purchased from Sigma-Aldrich (Darmstadt, Germany). The $8.6 \times 10^{-4} \text{ mol}\cdot\text{L}^{-1}$ stock solution of triclosan was prepared by dissolving TCS in ethanol: PB solution (1:3 *v/v*). The final concentration of TCS was achieved by diluting the stock solution with PB pH 7.4. DNA was dissolved in nanopure water to a concentration of $1 \text{ mg}\cdot\text{mL}^{-1}$. $[\text{Fe}(\text{CN})_6]^{3-/4-}$, Na_2HPO_4 and NaH_2PO_4 were obtained from Lachema (Řečkovice, Czech Republic). AgNPs were prepared using a chemical synthesis protocol described by Martínez-Castañón et al. [67]. Other chemicals of analytical reagent grade purity were purchased from Mikrochem (Pezinok, Slovakia) or Lachema (Czech Republic). Nanopure water with a resistivity of about $18 \text{ M}\Omega\cdot\text{cm}$ (Milipore Milli-Q system) was used for all experiments.

2.2. Apparatus

For all voltammetric experiments an Autolab PGSTAT12 potentiostat/galvanostat electrochemical system (Metrohm, Barendrecht, The Netherlands) driven by the software NOVA version 1.10.23 (Metrohm, Barendrecht, The Netherlands) was used. The three-electrode system consisted of a glassy carbon working electrode (GCE, Metrohm, Barendrecht, The Netherlands) with a disc diameter of 3 mm, Ag/AgCl/ $3 \text{ mol}\cdot\text{L}^{-1}$ KCl reference electrode and a platinum wire counter electrode (L-CHEM, Horka nad Moravou, Czech Republic). All measurements were performed in 20 mL glass cells at ambient temperature.

2.3. Preparation of the Biosensors

The GCE surface was mechanically cleaned on a polishing cloth (BUEHLER, London, UK) with $0.3 \mu\text{m}$ alumina suspension (Metrohm, Barendrecht, The Netherlands). GCE pretreatment was performed by polarization at a potential of 1.6 V for 300 s in $0.1 \text{ mol}\cdot\text{L}^{-1}$ PB solution of pH 7.4, and by stabilization of the CV response in $1 \times 10^{-3} \text{ M}$ $[\text{Fe}(\text{CN})_6]^{3-/4-}$ redox indicator in cycling within the potential range from 1.0 to -0.8 V for 15 scans. The electrode modification was carried out by covering the pretreated GCE surface with $4 \mu\text{L}$ of DNA solution. After drying for 20 min., the DNA/GCE biosensor was stabilized by an incubation in $0.1 \text{ mol}\cdot\text{L}^{-1}$ PB solution for 2 min. For the preparation of Ag/DNA/GCE biosensor, $4 \mu\text{L}$ of $1 \times 10^{-3} \text{ mol}\cdot\text{L}^{-1}$ AgNPs solution was dropped on the surface of the dry DNA/GCE biosensor and allowed to evaporate for 30 min. After 2 min. stabilization in PB solution, the Ag/DNA/GCE biosensor was used in the experiments.

2.4. Methods

2.4.1. Cyclic Voltammetry (CV)

CV scans were recorded within a potential range from 1.2 V to 0.0 V at a scan rate of $100 \text{ mV}\cdot\text{s}^{-1}$ and a potential step of 2 mV in $0.1 \text{ mol}\cdot\text{L}^{-1}$ PB or $1 \text{ mmol}\cdot\text{L}^{-1}$ $[\text{Fe}(\text{CN})_6]^{3-/4-}$ redox indicator in PB pH 7.4 with/without TCS in 20 mL electrochemical cell at laboratory temperature $21 \text{ }^\circ\text{C}$.

2.4.2. Square-Wave Voltammetry (SWV)

Square-wave voltammograms (SWV) were recorded under the following experimental conditions: potential step 4 mV, scan rate $200 \text{ mV}\cdot\text{s}^{-1}$, pulse amplitude 20 mV, frequency 50 Hz.

3. Results and Discussion

3.1. Characterization of the DNA/GCE Biosensor Stability

The first step in the preparation of the biosensor was the immobilization of DNA on the GCE working electrode, checked by the voltammetric response. A badly developed CV curve of the typical $[\text{Fe}(\text{CN})_6]^{3-/4-}$ redox indicator on the DNA modified electrode, compared to the bare GCE is known to be the result of an electrostatic repulsion of indicator

anions by the negatively charged surface-attached DNA backbone (Figure 1). Treatment of the newly prepared DNA/GCE biosensor in 1×10^{-3} mol·L⁻¹ redox indicator in PB pH 7.4 for selected time periods has been used to stabilize the DNA layer. The CV peak current values rise slightly with time of the biosensor incubation indicating an efficient and stable GCE coverage by DNA (Figure 1A).

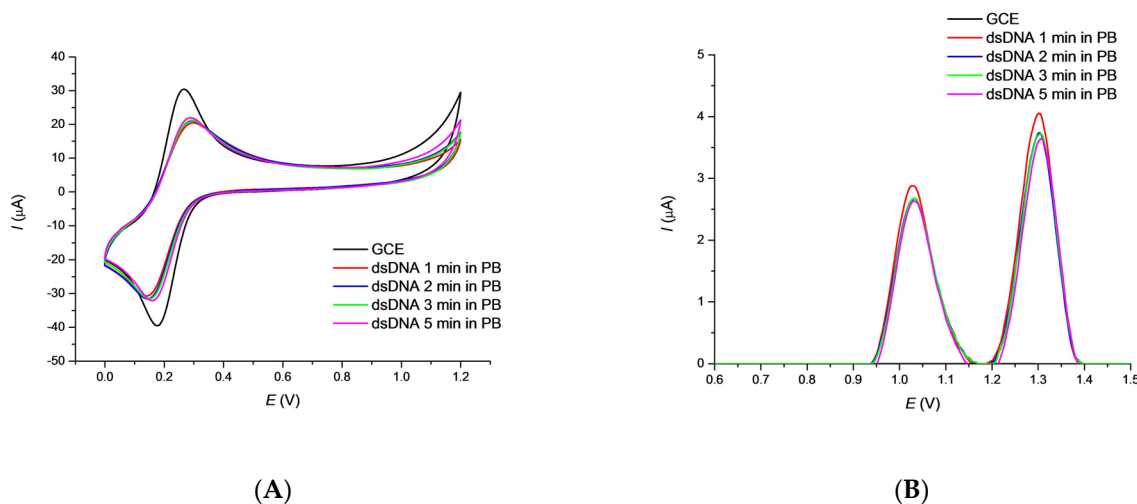


Figure 1. CV curves for 1×10^{-3} mol·L⁻¹ redox indicator (A) and SWV (B) curves obtained for the bare GCE and DNA/GCE biosensor in 0.1 mol·L⁻¹ PB pH 7.4 after treatment in the supporting electrolyte for a given time. Conditions: CV step potential 2 mV, scan rate 100 mV·s⁻¹; SWV amplitude 20 mV, frequency 50 Hz, step potential 4 mV and scan rate 200 mV·s⁻¹.

Square wave voltammetry (SWV) is a suitable electroanalytical method for the determination of both the triclosan and the guanine (G) and adenine (A) moieties. The optimization study revealed (data not shown) that the set of pulse amplitude of 20 mV, frequency of 50 Hz, step potential of 4 mV, and scan rate of 200 mV·s⁻¹ were best for monitoring. SWV peak currents of the G and A moieties decreased slightly within the given time intervals of the biosensor pretreatment in the supporting electrolyte (Figure 1B). As 2 min. treatment in PB solution was again the shortest time in which leaching of free DNA is nearly finished, it has been selected as appropriate for the newly prepared biosensor.

3.2. Effect of AgNPs on DNA/GCE Biosensor

To avoid the signal interferences of AgNPs with DNA, an optimization study with several dilutions of nanoparticle solutions was performed by a set of voltammetric experiments. Stock solutions of the corresponding 1×10^{-3} mol·L⁻¹ AgNPs were diluted 1:3, 1:5, and 1:10 (v/v) with PB pH 7.4 and dropped on the surface of DNA/GCE. After 30 min. incubation period and 2 min. biosensor treatment in 0.1 mol·L⁻¹ PB pH 7.4, SWV curves were recorded (Figure 2). The anodic peak potential values of 0.975 V and 1.251 V, E_{pG} and E_{pA} , were observed for the guanine (G) and adenine (A) moieties, respectively. The corresponding SWV current responses of the deoxynucleotides decreased with the concentration of nanoparticles applied. This decrease can be explained by a barrier effect for electron transfer evidently caused by an association of AgNPs with the dsDNA backbone as recently described [68]. Based on these results, the concentration of 1×10^{-4} mol·L⁻¹ Ag1 and Ag2 nanoparticles was chosen for ongoing measurements which corresponds to a 1:10 (v/v) dilution of nanoparticles stock solution with PB. This AgNPs concentration should protect the DNA layer by association and, at the same time, not interfere with the detection of an effect of TCS in a further study. No GCE surface passivation by AgNPs was detected under these conditions.

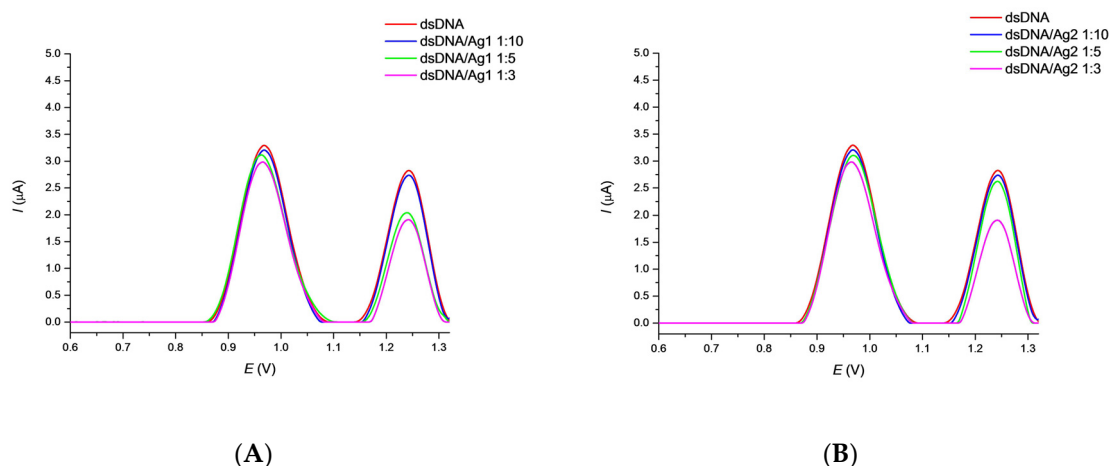


Figure 2. SWV curves recorded after 30 min. incubation of the DNA/GCE biosensor with Ag1 (A) and Ag2 (B) nanoparticles followed by 2 min. biosensor treatment in $0.1 \text{ mol}\cdot\text{L}^{-1}$ PB pH 7.4. SWV conditions: amplitude 20 mV, frequency 50 Hz, step potential 4 mV and scan rate $200 \text{ mV}\cdot\text{s}^{-1}$.

3.3. Effect of TCS on DNA/GCE Biosensor

The basic voltammetric behavior of TCS alone was previously described [65,69] and also confirmed in this work (data not shown). TCS exhibited the anodic response in the 0.57 V region vs. Ag/AgCl which depended on the TCS concentration within the range from 4×10^{-6} to $8 \times 10^{-5} \text{ mol}\cdot\text{L}^{-1}$. However, TCS degrades the DNA molecule in concentration and time depending manner and our study was further directed at the detection of DNA changes. The effect of TCS on DNA was monitored using the SWV responses of nucleobase moieties after an incubation of the biosensor in TCS solutions for 15 min under stirring (Figure 3). Within the increasing concentrations of TCS, the I_{pG} values significantly decrease while the E_{pG} values slightly shift from 0.975 V toward the less positive potential of 0.960 V. The I_{pA} response also decreases and the E_{pA} values shift from 1.251 V to 1.233 V. Additionally, a SWV response of a TCS residue was detected as a small wide peak in the potential region of 0.57 V (Figure 3). This is in agreement with [65] where a similar peak was observed depending on the pH of the medium used. Changes in nucleobases responses confirm damage to DNA by the TCS drug, accompanied by a partial liberation of nucleobases bonds in the helix [70].

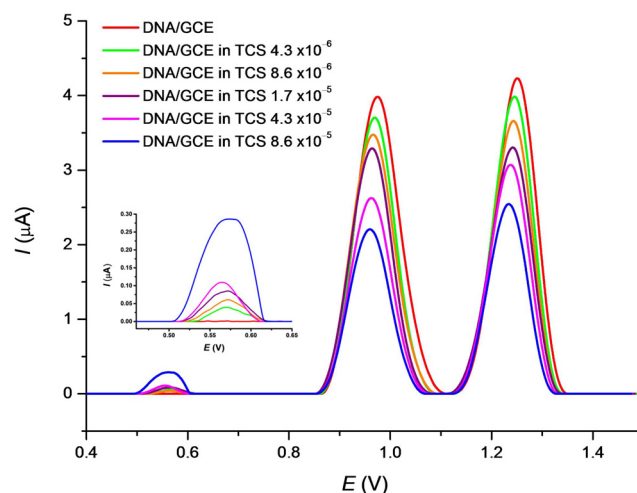


Figure 3. SWV curves recorded after 15 min. incubation of the DNA/GCE biosensor in TCS solutions of various concentration in $0.1 \text{ mol}\cdot\text{L}^{-1}$ PB pH 7.4. SWV conditions: amplitude 20 mV, frequency 50 Hz, step potential 4 mV and scan rate $200 \text{ mV}\cdot\text{s}^{-1}$.

3.4. Effect of TCS on Ag/DNA/GCE Biosensor

The mutual effect of TCS and AgNPs toward surface-attached DNA damage was tested using the Ag/DNA/GCE biosensor. The Ag1/DNA/GCE and Ag2/DNA/GCE biosensors were immersed in the TCS solution of various concentrations and allowed to incubate for 15 min under stirring. The SW voltammograms were then recorded immediately and directly in the TCS solution. In Figure 4A,B a decrease in the I_{pG} and I_{pA} values can be seen at both the Ag1/DNA/GCE and Ag2/DNA/GCE biosensors in proportion to increase in the triclosan concentration. The small E_{pG} shift to more negative potential values was observed only at Ag1/DNA/GCE. Again, the TCS residue can be observed as a slightly growing peak in the potential region of 0.57 V. The decrease in the I_{pG} response is less exhibited for Ag1/DNA/GCE. It is possible to conclude that both AgNPs used for the biosensor surface modification have protected the surface-attached DNA against its TCS-induced damage.

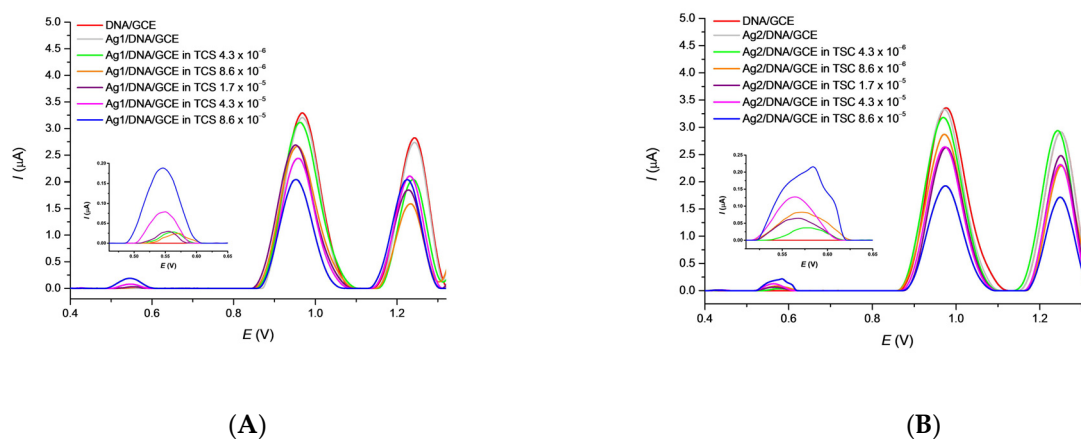


Figure 4. This SWV curves recorded after 15 min. incubation of the Ag1/DNA/GCE (A) and Ag2/DNA/GCE (B) biosensors in TCS solutions of various concentration in $0.1 \text{ mol}\cdot\text{L}^{-1}$ PB pH 7.4. SWV conditions: amplitude 20 mV, frequency 50 Hz, step potential 4 mV and scan rate $200 \text{ mV}\cdot\text{s}^{-1}$.

3.5. Protective Effect of AgNPs on DNA Damage by TCS

An overall comparison of a decrease in the fraction of survived dsDNA (expressed by the relative current response of the nucleobases moieties) with an increase in the TCS concentration in the absence and in the presence of Ag nanoparticles is depicted in Figure 5. In most cases, a protection of DNA by the immobilized AgNPs (red and green columns) is seen.

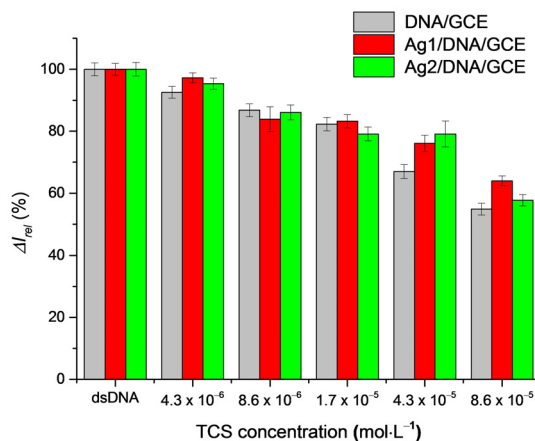


Figure 5. The amount of survived surface attached dsDNA expressed by its relative guanine moiety SWV peak current response in dependence on the concentration of TCS used at the 15 min incubation of DNA/GCE, Ag1/DNA/GCE and Ag2/DNA/GCE in TCS solutions.

The protective effect of AgNPs can be explained by their already reported direct interaction with the structure of dsDNA [68] and probably also by an interaction of TCS with AgNPs similarly to TiO₂ nanoparticles [71]. It seems that Ag1NPs with smaller dimensions (15 nm) adsorb on the dsDNA structure in a greater amount than Ag2NPs (37 nm), and somewhat better prevent the interaction of triclosan with dsDNA. DNA protection could be further improved using a higher amount of the Ag nanoparticles (i.e., a smaller dilution of the AgNPs solution such as 1:5).

4. Conclusions

DNA—drug interactions are of permanent interest, particularly for species that indicate potential damaging effects such as triclosan. In this study, the experimental conditions for examining the effects of TCS on surface-attached dsDNA were optimized and subsequently applied to the analysis of the DNA—TCS interaction with the electrochemical DNA/GCE biosensor. The negative effect of triclosan on DNA the helix structure was confirmed by monitoring the nucleobases responses. The silver nanoparticles immobilized over DNA exhibited some protection against TCS present in the solution phase, which revealed less damage to the DNA structure.

The results obtained here indicate a possibility of decreasing the toxic effect of TCS toward DNA by the presence of third species such as AgNPs. This can be of general interest in the case of a necessity of the elimination of unwanted effects of chemicals. For such further study we plan the investigation of morphology of the electrode surface modification as well as changes in the DNA structure using FTIR and Raman spectroscopies with special equipment allowing the measurement at the electrode body.

Author Contributions: J.B. proposed a design scheme for the biosensor with the tests performance and completed the paper. J.L. did the supervision and editing of the manuscript. All authors have read and agreed to the published version of the manuscript.

Funding: This research was supported by the Scientific Grant Agency of the Slovak Republic (VEGA Project No. 1/0159/20).

Institutional Review Board Statement: Not applicable.

Informed Consent Statement: Not applicable.

Data Availability Statement: Not applicable.

Conflicts of Interest: The authors declare no conflict of interest.

References

1. Oliver, M.; Kudlak, B.; Wiczerzak, M.; Reis, S.; Lima, S.A.C.; Segundo, M.A.; Miro, M. Ecotoxicological equilibria of triclosan in Microtox, XenoScreen YES/YAS, Caco2, HEPG2 and liposomal systems are affected by the occurrence of other pharmaceutical and personal care emerging contaminants. *Sci. Total Environ.* **2020**, *719*, 137358. [[CrossRef](#)]
2. WW-Chung, P.; Rafqah, S.; Vyard, G.; Sarakha, M. Photochemical behaviour of triclosan in aqueous solutions: Kinetic and analytical studies. *J. Photochem. Photobiol. A Chem.* **2007**, *191*, 201–208. [[CrossRef](#)]
3. Thompson, A.; Griffin, P.; Stuetz, R.; Cartmell, E. The fate and removal of triclosan during wastewater treatment. *Water Environ. Res.* **2005**, *77*, 63–67. [[CrossRef](#)]
4. Koepe, E.S.; Ferguson, K.K.; Colacino, J.A.; Meeker, J.D. Relationship between urinary Triclosan and paraben concentrations and serum thyroid measures in NHANES 2007–2008. *Sci. Total Environ.* **2013**, *445–446*, 299–305. [[CrossRef](#)]
5. Yueh, M.-F.; Tukey, R.H. Triclosan: A Widespread Environmental Toxicant with Many Biological Effects. *Annu. Rev. Pharmacol. Toxicol.* **2016**, *56*, 251–272. [[CrossRef](#)]
6. Falfushynska, H.I.; Gnatyshyna, L.L.; Osadchuk, O.Y.; Farkas, A.; Vehovszky, A.; Carpenter, D.O.; Gyori, J.; Stoliar, O.B. Diversity of the molecular responses to separate wastewater effluents in freshwater mussels. *Comp. Biochem. Physiol. Part C Toxicol. Pharmacol.* **2014**, *164*, 51–58. [[CrossRef](#)]
7. Carrouel, F.; Viennot, S.; Ottolenghi, L.; Gaillard, C.; Bourgeois, D. Nanoparticles as Anti-Microbial, Anti-Inflammatory, and Remineralizing Agents in Oral Care Cosmetics: A Review of the Current Situation. *Nanomaterials* **2020**, *10*, 140. [[CrossRef](#)]
8. Fu, J.; Gong, Z.; Bae, S. Assessment of the Effect of Methyl-Triclosan and Its Mixture with Triclosan on Developing Zebrafish (*Danio rerio*) Embryos Using Mass Spectrometry-Based Metabolomics. *J. Hazard. Mater.* **2019**, *368*, 186–196. [[CrossRef](#)]

9. Peng, F.J.; Hu, L.X.; Pan, C.G.; Ying, G.G.; Van den Brink, P.J. Insights into the Sediment Toxicity of Personal Care Products to Freshwater Oligochaete Worms Using Fourier Transform Infrared Spectroscopy. *Ecotoxicol. Environ. Saf.* **2019**, *172*, 296–302. [[CrossRef](#)]
10. Hovander, L.; Malmberg, T.; Athanasiadou, M.; Athanassiadis, I.; Rahm, S.; Bergman, A.; Wehler, E.K. Identification of hydroxylated PCB metabolites and other phenolic halogenated pollutants in human blood plasma. *Arch. Environ. Contam. Toxicol.* **2002**, *42*, 105–117. [[CrossRef](#)]
11. Calafat, A.M.; Ye, X.; Wong, L.Y.; Reidy, J.A.; Needham, L.L. Urinary Concentrations of Triclosan in the U.S. Population: 2003–2004. *Environ. Health Perspect.* **2008**, *116*, 303–307. [[CrossRef](#)]
12. Fang, J.L.; Stingley, R.L.; Beland, F.A.; Harrouk, W.; Lumpkins, D.L.; Howard, P. Occurrence, efficacy, metabolism, and toxicity of triclosan. *J. Environ. Sci. Health C Environ. Carcinog. Ecotoxicol. Rev.* **2010**, *28*, 147–171. [[CrossRef](#)] [[PubMed](#)]
13. Honkisz, E.; Zieba-Przybylska, D.; Wojtowicz, A.K. The effect of triclosan on hormone secretion and viability of human choriocarcinoma JEG-3 cells. *Reprod. Toxicol.* **2012**, *34*, 385–392. [[CrossRef](#)] [[PubMed](#)]
14. Geens, T.; Neels, H.; Covaci, A. Distribution of bisphenol-A, triclosan and n-nonylphenol in human adipose tissue, liver and brain. *Chemosphere* **2012**, *87*, 796–802. [[CrossRef](#)] [[PubMed](#)]
15. Wolff, M.S.; Teitelbaum, S.L.; Windham, G.; Pinney, S.M.; Britton, J.A.; Chelimo, C.; Godbold, J.; Biro, F.; Kushi, L.; Pfeiffer, C.M.; et al. Pilot study of urinary biomarkers of phytoestrogens, phthalates, and phenols in girls. *Environ. Health Perspect.* **2007**, *115*, 116–121. [[CrossRef](#)]
16. Rodricks, J.V.; Swenberg, J.A.; Borzelleca, J.F.; Maronpot, R.R.; Shipp, A.M. Triclosan: A critical review of the experimental data and development of margins of safety for consumer products. *Crit. Rev. Toxicol.* **2010**, *40*, 422–484. [[CrossRef](#)]
17. Yueh, M.F.; Taniguchi, K.; Chen, S.; Evans, R.M.; Hammock, B.D.; Karin, M.; Tukey, R.H. The commonly used antimicrobial additive triclosan is a liver tumor promoter. *Proc. Natl. Acad. Sci. USA* **2014**, *111*, 17200–17205. [[CrossRef](#)]
18. Szychowski, K.A.; Wnuk, A.; Kajta, M.; Wojtowicz, A.K. Triclosan activates aryl hydrocarbon receptor (AhR)-dependent apoptosis and affects Cyp1a1 and Cyp1b1 expression in mouse neocortical neurons. *Environ. Res.* **2016**, *151*, 106–114. [[CrossRef](#)]
19. Kim, J.; Oh, H.; Ryu, B.; Kim, U.; Lee, J.M.; Jung, C.R.; Kim, C.; Park, J.H. TCS affects axon formation in the neural development stages of zebrafish embryos (*Danio rerio*). *Environ. Pollut.* **2018**, *236*, 304–312. [[CrossRef](#)]
20. Park, B.K.; Gonzales, E.L.; Yang, S.M.; Bang, M.; Choi, C.S.; Shin, C.Y. Effects of triclosan on neural stem cell viability and survival. *Biol. Ther.* **2016**, *24*, 99–107. [[CrossRef](#)]
21. Wang, F.; Guo, X.; Chen, W.; Sun, Y.; Fan, C. Effects of triclosan on hormones and reproductive axis in female Yellow River carp (*Cyprinus carpio*): Potential mechanisms underlying estrogen effect. *Toxicol. Appl. Pharm.* **2017**, *336*, 49–54. [[CrossRef](#)] [[PubMed](#)]
22. Liu, J.; Sun, L.; Zhang, H.; Shi, M.; Dahlgren, R.A.; Wang, X.; Wang, H. Response mechanisms to joint exposure of triclosan and its chlorinated derivatives on zebrafish (*Danio rerio*) behavior. *Chemosphere* **2018**, *193*, 820–832. [[CrossRef](#)] [[PubMed](#)]
23. Arya, S.; Dwivedi, A.K.; Alvarado, L.; Kupesic-Plavsic, S. Exposure of U.S. population to endocrine disruptive chemicals (parabens, benzophenone-3, bisphenol-a and triclosan) and their associations with female infertility. *Environ. Pollut.* **2020**, *265*, 114763. [[CrossRef](#)] [[PubMed](#)]
24. Yee, A.L.; Gilbert, J.A. Is triclosan harming your microbiome? *Science* **2016**, *353*, 348–349. [[CrossRef](#)] [[PubMed](#)]
25. Jutkina, J.; Marathe, N.P.; Flach, C.F.; Larsson, D.G.J. Antibiotics and common antibacterial biocides stimulate horizontal transfer of resistance at low concentrations. *Sci. Total Environ.* **2018**, *616*, 172–178. [[CrossRef](#)]
26. Lu, J.; Wang, Y.; Zhang, S.; Bond, P.; Yuan, Z.; Guo, J. Triclosan at environmental concentrations can enhance the spread of extracellular antibiotic resistance genes through transformation. *Sci. Total Environ.* **2020**, *713*, 136621. [[CrossRef](#)]
27. Sanidad, K.Z.; Xiao, H.; Zhang, G. Triclosan, a common antimicrobial ingredient, on gut microbiota and gut health. *Gut. Microbes* **2019**, *10*, 434–437. [[CrossRef](#)]
28. Ruszkiewicz, J.A.; Li, S.; Rodriguez, M.B.; Aschner, M. Is triclosan a neurotoxic agent? *J. Toxicol. Environ. Health B Crit. Rev.* **2017**, *20*, 104–117. [[CrossRef](#)]
29. Bertelsen, R.J.; Longnecker, M.P.; Lovik, M.; Calafat, A.M.; Carlsen, K.H.; London, S.J.; Lødrup Carlsen, K.C. Triclosan exposure and allergic sensitization in Norwegian children. *Allergy* **2013**, *68*, 84–91. [[CrossRef](#)]
30. Wang, X.; Zou, L.; Mi, C.; Yu, H.; Dong, M.; Teng, Y. Characterization of binding interaction of triclosan and bovine serum albumin. *J. Environ. Sci. Health A* **2020**, *55*, 318–325. [[CrossRef](#)]
31. Roszak, J.; Smok-Pieniazek, A.; Spryszynska, S.; Kowalczyk, K.; Domeradzka-Gajda, K.; Swiercz, R.; Grobelny, J.; Tomaszewska, E.; Ranoszek-Soliwoda, K.; Celichowski, G.; et al. Cytotoxic effects in transformed and non-transformed human breast cell lines after exposure to silver nanoparticles in combination with selected aluminium compounds, parabens or phthalates. *J. Hazard. Mater.* **2020**, *392*, 122442. [[CrossRef](#)] [[PubMed](#)]
32. Bondarenko, O.; Juganson, K.; Ivask, A.; Kasemets, K.; Mortimer, M.; Kahru, A. Toxicity of Ag, CuO and ZnO Nanoparticles to Selected Environmentally Relevant Test Organisms and Mammalian Cells In Vitro: A Critical Review. *Arch. Toxicol.* **2013**, *87*, 1181–1200. [[CrossRef](#)] [[PubMed](#)]
33. Ahamed, M.; AlSalhi, M.S.; Siddiqui, M.K.J. Silver Nanoparticle Applications and Human Health. *Clin. Chim. Acta* **2010**, *411*, 1841–1848. [[CrossRef](#)]
34. Vance, M.E.; Kuiken, T.; Vejerano, E.P.; McGinnis, S.P.; Hochella, M.F.; Rejeski, D.; Hull, M.S. Nanotechnology in the Real World: Redeveloping the Nanomaterial Consumer Products Inventory. *Beilstein J. Nanotechnol.* **2015**, *6*, 1769–1780. [[CrossRef](#)] [[PubMed](#)]

35. Li, M.; Zhang, C.H. Are silver nanoparticles better than triclosan as a daily antimicrobial? Answers from the perspectives of gut microbiome disruption and pathogenicity. *Sci. Total Environ.* **2021**, *756*, 143983. [[CrossRef](#)] [[PubMed](#)]
36. Prabhu, S.; Poulouse, E.K. Silver nanoparticles: Mechanism of antimicrobial action, synthesis, medical applications, and toxicity effects. *Int. Nano Lett.* **2012**, *2*, 32. [[CrossRef](#)]
37. Gaillet, S.; Rouanet, J.-M. Silver nanoparticles: Their potential toxic effects after oral exposure and underlying mechanisms—A review. *Food Chem. Toxicol.* **2015**, *77*, 58–63. [[CrossRef](#)] [[PubMed](#)]
38. Do Nascimento, C.; Paulo, D.F.; Pita, M.S.; Pedrazzi, V.; de Albuquerque Junior, R.F. Microbial diversity of the supra- and subgingival biofilm of healthy individuals after brushing with chlorhexidine- or silver-coated toothbrush bristles. *Can. J. Microbiol.* **2015**, *61*, 112–123. [[CrossRef](#)]
39. Mackevica, A.; Olsson, M.E.; Hansen, S.F. The release of silver nanoparticles from commercial toothbrushes. *J. Hazard. Mater.* **2017**, *322*, 270–275. [[CrossRef](#)]
40. Li, Y.; Cummins, E. Hazard characterization of silver nanoparticles for human exposure routes. *J. Environ. Sci. Health A* **2020**, *55*, 704–725. [[CrossRef](#)]
41. Shang, L.; Nienhaus, K.; Nienhaus, G.U. Engineered nanoparticles interacting with cells: Size matter. *J. Nanobiotechnol.* **2014**, *12*, 5. [[CrossRef](#)]
42. Park, E.J.; Bae, E.; Yi, J.; Kim, Y.; Choi, K.; Lee, S.H.; Yoon, J.; Lee, B.C.; Park, K. Repeated-Dose Toxicity and Inflammatory Responses in Mice by Oral Administration of Silver Nanoparticles. *Environ. Toxicol. Pharmacol.* **2010**, *30*, 162–168. [[CrossRef](#)]
43. Anderson, D.S.; Silva, R.M.; Lee, D.; Edwards, P.C.; Sharmah, A.; Guo, T.; Pinkerton, K.E.; Van Winkle, L.S. Persistence of Silver Nanoparticles in the Rat Lung: Influence of Dose, Size, and Chemical Composition. *Nanotoxicology* **2015**, *9*, 591–602. [[CrossRef](#)] [[PubMed](#)]
44. Li, J.; Tang, M.; Xue, Y. Review of the effects of silver nanoparticle exposure on gut bacteria. *J. Appl. Toxicol.* **2019**, *39*, 27–37. [[CrossRef](#)] [[PubMed](#)]
45. Van den Brule, S.; Ambroise, J.; Lecloux, H.; Levard, C.; Soulas, R.; De Temmerman, P.-J.; Palmari-Pallag, M.; Marbaix, E.; Lison, D. Dietary silver nanoparticles can disturb the gut microbiota in mice. *Part. Fibre Toxicol.* **2016**, *13*, 38. [[CrossRef](#)] [[PubMed](#)]
46. Simko, M.; Fiedeler, U.; Gazsó, A.; Nentwich, M. The impact of nanoparticles on cellular functions. *Nano Trust-Dossier* **2011**, *7*, 151–164.
47. Panacek, A.; Kvítek, L.; Pucek, R.; Kolar, M.; Vecerova, R.; Pizúrova, N.; Sharma, V.K.; Nevecna, T.; Zboril, R. Silver colloid nanoparticles: Synthesis, characterization, and their antibacterial activity. *J. Phys. Chem. B* **2006**, *110*, 16248–16253. [[CrossRef](#)]
48. Morones, J.R.; Elechiguerra, J.L.; Camacho, A.; Holt, K.; Kouri, J.B.; Ramírez, J.T.; Yacaman, M.J. The bactericidal effect of silver nanoparticles. *Nanotechnology* **2005**, *16*, 2346–2353. [[CrossRef](#)]
49. Qasim, M.; Udomluck, N.; Chang, J.; Park, H.; Kim, K. Antimicrobial activity of silver nanoparticles encapsulated in poly-N-isopropylacrylamide-based polymeric nanoparticles. *Int. J. Nanomed.* **2018**, *13*, 235–249. [[CrossRef](#)]
50. Sotiriou, G.A.; Pratsinis, S.E. Antibacterial activity of nanosilver ions and particles. *Environ. Sci. Technol.* **2010**, *44*, 5649–5654. [[CrossRef](#)]
51. Nateghi, M.R.; Hajimirzababa, H. Effect of silver nanoparticles morphologies on antimicrobial properties of cotton fabrics. *J. Text. Inst.* **2014**, *105*, 806–813. [[CrossRef](#)]
52. Lkhagvajav, N.; Koizhaiganova, M.; Yasa, I.; Çelik, E.; Sari, Ö. Characterization and antimicrobial performance of nano silver coatings on leather materials. *Braz. J. Microbiol.* **2015**, *46*, 41–48. [[CrossRef](#)] [[PubMed](#)]
53. Davenport, L.L.; Hsieh, H.; Eppert, B.L.; Carreira, V.S.; Krishan, M.; Ingle, T.; Howard, P.C.; Williams, M.T.; Vorhees, C.V.; Genter, M.B. Systemic and Behavioral Effects of Intranasal Administration of Silver Nanoparticles. *Neurotoxicol. Teratol.* **2015**, *51*, 68–76. [[CrossRef](#)] [[PubMed](#)]
54. Ghaderi, S.; Tabatabaei, S.R.F.; Varzi, H.N.; Rashno, M. Induced Adverse Effects of Prenatal Exposure to Silver Nanoparticles on Neurobehavioral Development of Offspring of Mice. *J. Toxicol. Sci.* **2015**, *40*, 263–275. [[CrossRef](#)]
55. Tak, Y.K.; Pal, S.; Naoghare, P.K.; Rangasamy, S.; Song, J.M. Shape-Dependent Skin Penetration of Silver Nanoparticles: Does It Really Matter? *Sci. Rep.* **2015**, *5*, 16908. [[CrossRef](#)]
56. Queckenberg, C.; Meins, J.; Wachall, B.; Doroshenko, O.; Tomalik-Scharte, D.; Bastian, B.; Abdel-Tawab, M.; Fuhr, U. Absorption, pharmacokinetics, and safety of triclosan after dermal administration. *Antimicrob. Agents Chemother.* **2010**, *54*, 570–572. [[CrossRef](#)]
57. Sandborgh-Englund, G.; Adolfsson-Erici, M.; Odham, G.; Ekstrand, J. Pharmacokinetics of triclosan following oral ingestion in humans. *J. Toxicol. Environ. Health Part A* **2006**, *69*, 1861–1873. [[CrossRef](#)]
58. Weatherly, L.M.; Nelson, A.J.; Shim, J.; Riitano, A.M.; Gerson, E.D.; Hart, A.J.; de Juan-Sanz, J.; Ryan, T.A.; Sher, R.; Hess, S.T.; et al. Antimicrobial agent triclosan disrupts mitochondrial structure, revealed by super-resolution microscopy, and inhibits mast cell signaling via calcium modulation. *Toxicol. Appl. Pharmacol.* **2018**, *349*, 39–54. [[CrossRef](#)]
59. Alfihili, M.A.; Hindawi, M.-H.L. Review Article Triclosan: An Update on Biochemical and Molecular Mechanisms. *Oxid. Med. Cell. Longev.* **2019**, *2019*, 1607304. [[CrossRef](#)]
60. Ma, H.; Zheng, L.; Li, Y.; Pan, S.; Hu, J.; Yu, Z.; Zhang, G.; Sheng, G.; Fu, J. Triclosan reduces the levels of global DNA methylation in HepG2 cells. *Chemosphere* **2013**, *90*, 1023–1029. [[CrossRef](#)]
61. Binelli, A.; Cogni, D.; Parolini, M.; Riva, C.; Provini, A. Cytotoxic and genotoxic effects of in vitro exposure to triclosan and trimethoprim on zebra mussel (*Dreissena polymorpha*) hemocytes. *Comp. Biochem. Physiol. Part C Toxicol. Pharmacol.* **2009**, *150*, 50–56. [[CrossRef](#)] [[PubMed](#)]

62. Lovecka, P.; Macurkova, A.; Zaruba, K.; Hubacek, T.; Siegel, J.; Valentova, O. Genomic Damage Induced in *Nicotiana tabacum* L. Plants by Colloidal Solution with Silver and Gold Nanoparticles. *Plants* **2021**, *10*, 1260. [[CrossRef](#)] [[PubMed](#)]
63. Kurbanoglu, S.; Dogan-Topal, B.; Hlavata, L.; Labuda, J.; Ozkan, S.A.; Uslu, B. Electrochemical investigation of an interaction of the antidepressant drug aripiprazole with original and damaged calf thymus dsDNA. *Electrochim. Acta* **2015**, *169*, 233–240. [[CrossRef](#)]
64. Blaskovicova, J.; Sochr, J.; Koutsogiannis, A.; Diamantidou, D.; Kopel, P.; Adam, V.; Labuda, J. Detection of ROS Generated by UV-C Irradiation of CdS quantum Dots and their Effect on Damage to Chromosomal and Plasmid DNA. *Electroanalysis* **2018**, *30*, 698–704. [[CrossRef](#)]
65. Silva, E.H.C.; Lopes, I.C.; Bruzaca, E.E.S.; de Carvalho, P.A.V.; Tanaka, A.A. Triclosan: Electrochemistry, Spontaneous Degradation and Effects on Double-Stranded DNA. *Braz. J. Anal. Chem.* **2021**, *8*, 89–102. [[CrossRef](#)]
66. Talebpour, Z.; Haghighi, F.; Taheri, M.; Hosseinzadeh, M.; Gharavi, S.; Habibi, F.; Aliahmadi, A.; Sadr, A.S.; Azad, J. Binding interaction of spherical silver nanoparticles and calf thymus DNA: Comprehensive multispectroscopic, molecular docking, and RAPD PCR studies. *J. Mol. Liquids* **2019**, *289*, 111185. [[CrossRef](#)]
67. Martinez-Castanon, G.A.; Niño-Martínez, N.; Martínez-Gutierrez, F.; Martínez-Mendoza, J.R.; Ruiz, F. Synthesis and antibacterial activity of silver nanoparticles with different sizes. *J. Nanopart. Res.* **2008**, *10*, 1343–1348. [[CrossRef](#)]
68. Nemcekova, K.; Svitkova, V.; Sochr, J.; Gemeiner, P.; Labuda, J. Gallic acid-coated silver nanoparticles as perspective drug nanocarriers: Bioanalytical study. *Anal. Bioanal. Chem.* **2022**, 1–13. [[CrossRef](#)]
69. Yola, M.L.; Atar, N.; Eren, T.; Karimi-Malehc, H.; Wang, S. Sensitive and selective determination of aqueous triclosan based on gold nanoparticles on polyoxometalate/reduced graphene oxide nano hybrid. *RSC Adv.* **2015**, *5*, 65953. [[CrossRef](#)]
70. Peropadre, A.; Blanco, L.; Freire, P.F.; Repetto, G.; Hazen, M. Exposure to low doses of triclosan induces DNA-damage and increased proliferation in human keratinocytes. *Toxicol. Lett.* **2016**, *258*, S248. [[CrossRef](#)]
71. Stamatis, N.; Antonopoulou, M.; Hela, D.; Konstantinou, I. Photocatalytic degradation kinetics and mechanisms of antibacterial triclosan in aqueous TiO₂ suspensions under simulated solar irradiation. *J. Chem. Technol. Biotechnol.* **2014**, *89*, 1145–1154. [[CrossRef](#)]